ADBA
Computers and Electronics in Medicine
Cutting-Edge Scientific Solutions

e-ISSN: 3023-8609
RESEARCH ARTICLE
Vol.2 / No.2 / 2025 / pp.36-42
https://doi.org/10.69882/adba.cem.2025072

A Modified Transmission Line Modelling Approach for Bioheat Transfer

Burak Arıcıoğlu [*,α,1] **and Abdullah Ferikoğlu** [*,2]

*Faculty of Technology, Electrical-Electronics Engineering, Sakarya University of Applied Sciences, Serdivan, Türkiye, αBiomedical Technologies Application and Research Center (Biyotam), Sakarya University of Applied Sciences, Serdivan, Türkiye.

ABSTRACT This study presents a modified Transmission Line Modelling (TLM) method for simulating bioheat transfer in biological tissues, with a particular focus on accounting for non-unidirectional blood flow. While the Pennes bioheat equation has been widely used for such problems, it assumes unidirectional perfusion and may overlook important thermal effects introduced by non-unidirectional blood flow. To address this limitation, a TLM-based formulation of the Klinger bioheat equation known for incorporating flow directionality is developed and implemented for one-dimensional (1D) problems. A novel TLM cell model is introduced to represent the governing equation and its associated boundary conditions. Validation is performed through a 1D multilayer human tissue model exposed to electromagnetic (EM) fields at multiple 4G carrier frequencies. Comparative results with the Finite Element Method (FEM) show strong agreement, especially under steady-state conditions. Furthermore, the proposed model reveals that the impact of non-unidirectional blood flow becomes more pronounced in thicker tissue layers, confirming the importance of incorporating convective terms. This work demonstrates that the modified TLM approach provides a stable, efficient, and more physiologically accurate method for bioheat simulations.

KEYWORDS
TLM
Bioheat transfer
Klinger bioheat equation
Pennes bioheat equation

INTRODUCTION

Bioheat transfer plays a critical role in understanding thermal interactions within biological tissues (Singh 2024; Ostadhossein and Hoseinzadeh 2024), with wide-ranging applications in medical diagnostics (D'Alessandro *et al.* 2024; Akulova and Sheremet 2024), hyperthermia-based therapies (Jiang 2024; Sherief *et al.* 2024), and cryosurgery studies (Barman *et al.* 2021; Kumar and Rai 2022) among others. Traditional models, such as Pennes' bioheat equation (Pennes 1948), have provided a foundational framework for analysing heat conduction in perfused tissues. However, these models often assume simplified blood flow patterns, typically unidirectional and spatially averaged perfusion, which may not adequately capture the complexity of heat transmission in biological tissues (Hristov 2019; Tucci *et al.* 2021).

The Transmission Line Modelling (TLM) method has gained attention in the literature as a robust numerical technique for solving the wave equation, the diffusion equation and the linear combination of both wave and diffusion types of partial differential equations (PDEs) (Christopoulos and Christopoulos 1995; Aricioglu and Ferikoglu 2021; Johns 1977). A key advantage of the TLM method lies in its unconditional stability and the fact that it does not require matrix inversion for time-domain solutions, making it both efficient and scalable for large and complex simulations (Milan and Gebremedhin 2018).

In this study, a modified TLM method is presented for simulating bioheat transfer, extending the classical framework by incorporating non-unidirectional blood flow effects. The Pennes bioheat equation is one of the most commonly used models in the literature for solving bioheat transfer problems (Ostadhossein and Hoseinzadeh 2022; Abro *et al.* 2021; El-Sapa *et al.* 2024; Ezzat *et al.* 2014; Ferras *et al.* 2015). However, as noted by H.G. Klinger, the Pennes equation neglects the effects of non-unidirectional blood flow, which may lead to inaccuracies (Klinger 1974). Therefore, this study employs the Klinger bioheat equation as an alternative. To implement this, a new TLM cell model was developed that accounts for non-unidirectional blood flow. To the best of the author's knowledge, there is currently no TLM-based implementation of the Klinger bioheat equation in the literature. Thus, the TLM model for the Klinger equation constitutes the novel contribution of this work. For simplicity, only the one-dimensional (1D) case is considered.

The remainder of the paper is organized as follows: Section 2 presents the materials and methods. Section 3 provides numerical simulations and results. Finally, Section 4 concludes the paper with a summary of findings and perspectives for future work.

MATERIALS AND METHODS

In this section, the application of the TLM method to 1D bioheat problems is explained. The TLM method can be used to solve wave equations, diffusion equations, or any combination of the two. The general thermal diffusion equation is:

Manuscript received: 15 April 2025,
Revised: 24 May 2025,
Accepted: 5 July 2025.

[1]baricioglu@subu.edu.tr (**Corresponding author**)
[2]af@subu.edu.tr

$$k\nabla^2 T = \rho C\frac{\partial T}{\partial t} - Q. \tag{1}$$

Here, k is the thermal conductivity (W/mK), T is the temperature (K), ρ is the density (kg/m^3), C is the specific heat capacity (J/kgK), and Q is the heat source term (W/m^3). In biological tissues, thermal diffusion described by the Pennes bioheat equation is given by (Pennes 1948)

$$k_T\nabla^2 T = \rho_T C_T\frac{\partial T}{\partial t} + \omega_b C_b(T - T_b) - Q_{\text{met}} - Q_e. \tag{2}$$

Here, k_T is the thermal conductivity of the tissue (W/m·K), T is the temperature (K), ρ_T is the tissue density (kg/m^3), C_T is the specific heat capacity of the tissue (J/kg·K), ω_b is the blood perfusion rate (kg/m^{3}s), C_b is the specific heat capacity of blood (J/kg·K), T_b is the initial temperature of blood (K), Q_met is the metabolic heat generation rate (W/m^3), and Q_e is the power absorbed by the tissue from an external heat source (W/m^3). The Klinger bioheat equation is (Klinger 1974):

$$k_T\nabla^2 T = \rho_T C_T\frac{\partial T}{\partial t} + (\rho_T C_T)(\vec{u}\cdot\nabla T) - Q_{\text{met}} - Q_e. \tag{3}$$

The term $(\rho_T C_T)(\vec{u}\cdot\nabla T)$ represents the effect of blood flow velocity on heat distribution within the tissue, where $\vec{u}$ is the velocity vector (m/s). In this model, the physical properties of the tissue are assumed to be constant, and the blood flow is considered as an incompressible.

The new transmission line model for Klinger bioheat equation

The 1D transmission line that models the Klinger bioheat equation is shown in Figure 1

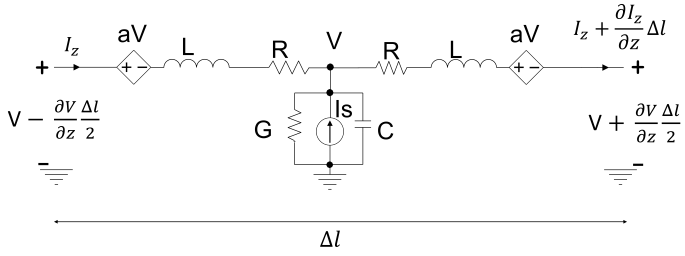

Figure 1 The 1D TLM circuit for the Klinger bioheat model.

In Figure 1, the current source models the metabolic and other heat sources (Milan and Gebremedhin 2018; Desai *et al.* 1992; Milan *et al.* 2014; Milan and Gebremedhin 2016), while the voltage-controlled voltage source represents the effect of blood flow on the bioheat distribution. Applying the Kirchhoff's Voltage Law (KVL) to the circuit in Figure 1 yields.

$$V - \frac{\partial V}{\partial z}\frac{\Delta l}{2} - aV - L\frac{\Delta l}{2}\frac{\partial I_z}{\partial t} - R\frac{\Delta l}{2}I_z - V = 0. \tag{4}$$

If (4) is rearranged and both sides of the equation are divided by $\Delta l/2$, then the following is obtained

$$-\frac{\partial V}{\partial z} - \frac{2a}{\Delta l}V = L\frac{\partial I_Z}{\partial t} + RI_Z. \tag{5}$$

Applying Kirchhoff's Current Law (KCL) at node V in Figure 1 gives:

$$I_Z - \left(I_Z + \frac{\partial I_Z}{\partial z}\frac{\Delta l}{2}\right) - \left(G\frac{\Delta l}{2}V + C\frac{\Delta l}{2}\frac{\partial V}{\partial t} - I_S\right) = 0. \tag{6}$$

If (6) is rearranged and both sides are divided by $\frac{\Delta l}{2}$ yields:

$$\frac{\partial I_Z}{\partial z} = -GV - C\frac{\partial V}{\partial t} + \frac{2I_S}{\Delta l}. \tag{7}$$

Taking the derivative of (5) with respect to z, and the derivative of (7) with respect to t, then combining the two yields:

$$\frac{\partial^2 V}{\partial z^2} = LC\frac{\partial^2 V}{\partial t^2} + (LG + RC)\frac{\partial V}{\partial t} + RGV + \frac{2a}{\Delta l}\frac{\partial V}{\partial z} - \frac{L}{\Delta l}\frac{\partial I_S}{\partial t} - \frac{RI_S}{\Delta l}. \tag{8}$$

(8) contains both wave and diffusion terms. Since the bioheat equation is fundamentally a diffusion equation, the diffusion terms should dominate. This is ensured by the condition: $LG + RC \gg \omega LC$ where R, L, G, and C denote the resistance, inductance, conductivity, and capacitance per unit length of the transmission line, and ω is the angular frequency. A simple way to satisfy this condition is by setting $L = 0$, which eliminates the wave term in (8). When $L = 0$, (8) simplifies to:

$$\frac{\partial^2 V}{\partial z^2} = RC\frac{\partial V}{\partial t} + RGV + \frac{2a}{\Delta l}\frac{\partial V}{\partial z} - \frac{RI_S}{\Delta l}. \tag{9}$$

By comparing (3) with (9), the equivalence relations shown in Table 1 can be established.

For the transmission line shown in Figure 1, the resistance R is selected as $1/k_T$. The remaining lumped parameters are then calculated accordingly, based on this choice. The corresponding values of the lumped elements for the 1D transmission line, expressed in terms of the tissue's thermal properties, are summarized in Table 2.

Boundary Condition Models in the TLM Used for Bioheat Problems

Heat transfer problems, including those involving bioheat transfer, typically involve four types of boundary conditions: interface boundary conditions, Dirichlet boundary conditions, Neumann boundary conditions, and convection boundary conditions. For simplicity in modeling these conditions, the effect of blood flow velocity on heat transfer is neglected at the boundaries.

Interface Boundary Condition The interface boundary condition is used in structures composed of multiple different materials. For the interface boundary condition to be valid, the following two conditions must be satisfied:

- The surfaces of the two different materials in contact must be at the same temperature.
- The interface must not store any energy.

The interface boundary condition can be defined as in (10).

$$-k_{T1}\frac{\partial T_1}{\partial x} = -k_{T2}\frac{\partial T_2}{\partial x}. \tag{10}$$

Here, k_{T1} and k_{T2} represent the thermal conductivities of two different tissues, while T_1 and T_2 denote the temperature distributions in the two different tissues. This boundary condition demonstrates the applicability of the TLM method in solving bioheat transfer equations for heterogeneous media. When examining the equivalencies given in Table 2, it is observed that the inverse of thermal conductivity is the R parameter of the transmission line, while the voltage corresponds to temperature. Therefore, when applying (10), the interface boundary condition can be represented as shown in Figure 2.

In Figure 2, at the surface where the two tissues are in contact, i.e., where the transmission line models are connected, the voltages

Table 1 Equivalence between the 1D Transmission Line and Klinger Bioheat Equation.

1D Transmission Line	Klinger Bioheat Equation
V (V)	T (K)
RC (Ω·F/m^2)	$\frac{\rho_T C_T}{k_T}$ (J·kg/m^3)
$\frac{2a}{\Delta l}$ (1/m)	$\frac{\rho_T C_T \lvert\vec{u}\rvert}{k_T}$ (W/kg·m^2)
RG (1/m^2)	$\frac{\omega_b C_b}{k_T}$ (W/m^3·K)
$\frac{I_S R}{\Delta l}$ (V/m^2)	$\frac{\omega_b C_b T_b + Q_{\text{met}} + Q_e}{k_T}$ (K/m^2)

Table 2 Equivalence between 1D Transmission Line Lumped Parameters and Thermal Properties dependent Parameters of Tissue.

1D Transmission Line Lumped Parameters	Thermal Properties dependent Parameters of Tissue
R (Ω/m)	$\frac{1}{k_T}$ (K·m/W)
C (F/m)	$\rho_T C_T$ (J/m^3·K)
G (1/Ω/m)	$\omega_b C_b$ (W/m^3·K)
$2a$	$\frac{\rho_T C_T \lvert\vec{u}\rvert \Delta l}{k_T}$
I_S (A)	$(\omega_b C_b T_b + Q_{\text{met}} + Q_e)\Delta l$ (W/m^2)

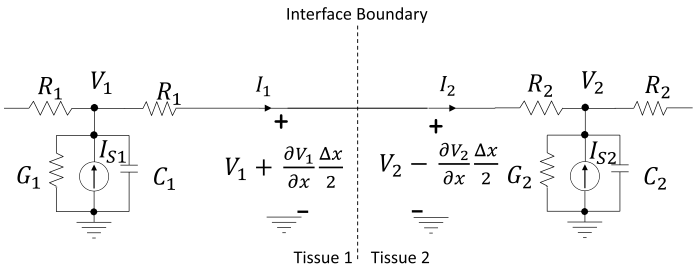

Figure 2 The circuit model for interface boundary condition in the TLM.

are equal, and there is no circuit element that stores energy at the interface. This satisfies the two conditions required for the interface boundary condition. The currents I_1 and I_2 in the figure are equal and can be calculated as in (11).

$$\begin{aligned} I_1 &= -\frac{1}{R_1}\frac{\partial V_1}{\partial x}, \\ I_2 &= -\frac{1}{R_2}\frac{\partial V_2}{\partial x}, \\ I_1 = I_2 &= -\frac{1}{R_1}\frac{\partial V_1}{\partial x} = -\frac{1}{R_2}\frac{\partial V_2}{\partial x}. \end{aligned} \tag{11}$$

Dirichlet Boundary Condition In heat transfer problems, the Dirichlet boundary condition indicates that the surface temperature remains constant. An example of this boundary condition occurs when the surface is in contact with a melting solid or a boiling liquid. In both cases, heat transfer occurs at the contact surface, but the surface temperature remains constant as the solid or liquid undergoes phase change.

In bioheat transfer problems, the Dirichlet boundary condition can be implemented in the TLM method by connecting a fixed voltage source at the end of the TLM cell to satisfies the Dirichlet condition. The modelling of this boundary condition is shown in Figure 3.

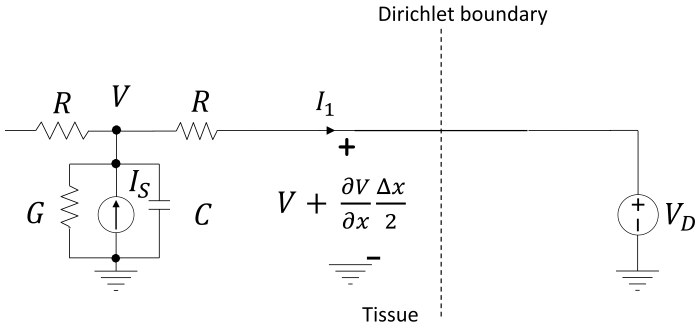

Figure 3 The circuit model for the Dirichlet boundary condition in the TLM.

Neumann Boundary Condition In heat transfer problems, the Neumann boundary condition is applied when the rate of temperature change, or the heat flux, at the boundary surface is known. This situation is mathematically expressed as in (12).

$$q_y = -k_T \frac{\partial T}{\partial x}. \tag{12}$$

Here, q_y is the heat flux at the boundary surface (W/m), and k_T is the thermal conductivity of the tissue (W/m·K). The Neumann boundary condition in the TLM model is shown in Figure 4.

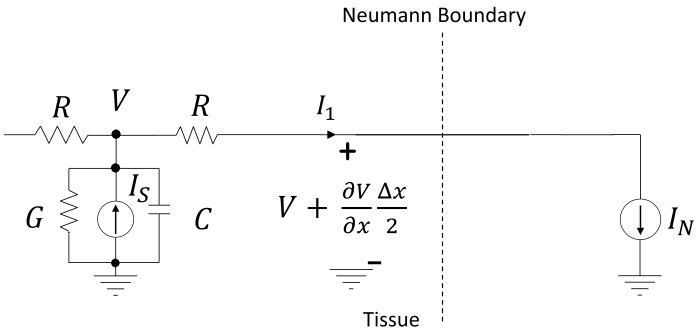

Figure 4 The circuit model for the Neumann boundary condition in the TLM.

In Figure 4, I_1 and I_N are equal, and can be calculated as follows:

$$I_1 = I_N = -\frac{1}{R}\frac{\partial V}{\partial x}. \tag{13}$$

In the Neumann boundary condition, the case where the heat flux at the boundary surface is zero is a special case and is also referred to as the insulated (adiabatic) boundary condition. This situation is mathematically expressed as in (14).

$$q_y = -k_T\frac{\partial T}{\partial x} = 0. \tag{14}$$

The adiabatic boundary condition in the TLM model is shown in Figure 5. In the figure, since the transmission line is terminated with an open circuit, the value of current I_1 is zero. Thus, the condition given in (14) is satisfied.

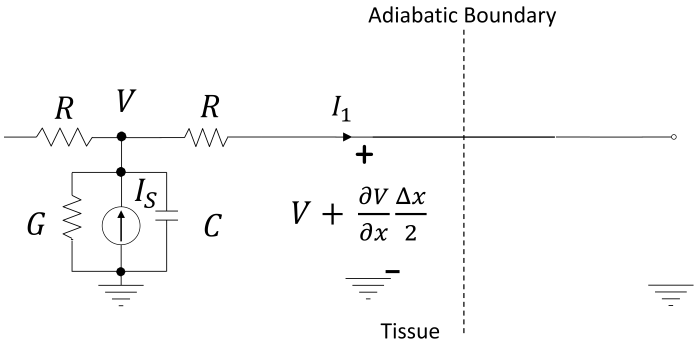

Figure 5 The circuit model for the adiabatic boundary condition in the TLM.

Convection Boundary Condition In heat transfer problems, the convection boundary condition is also known as Newton's boundary condition states that the heat transfer at the boundary surface is obtained from the conservation of energy at the surface. It is assumed that no energy is stored at the boundary surface. Therefore, the net heat flux entering the surface is equal to the net heat flux leaving the surface. Mathematically, the convection boundary condition is expressed as in (15).

$$-k_T\frac{\partial T}{\partial x} = h(T_T - T). \tag{15}$$

Here, k_T is the thermal conductivity of the tissue (W/m·K), T is the temperature in the tissue (K), h is the heat transfer coefficient at the boundary surface (W/m), and T_T is the temperature on the other side of the boundary surface. The model for the convection boundary condition is shown in Figure 6.

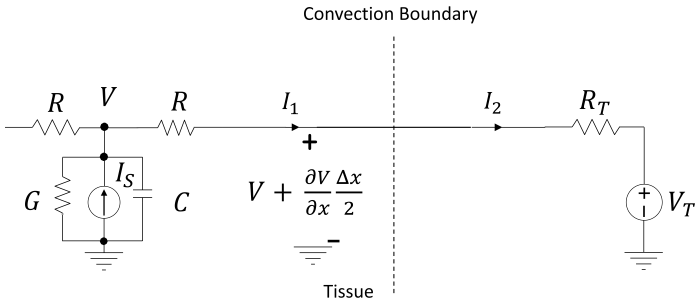

Figure 6 The circuit model for the convection boundary condition in the TLM model.

In Figure 6, the currents I_1 and I_2 are equal and can be written as follows.

$$\begin{aligned} I_1 &= -\frac{1}{R}\frac{\partial V}{\partial x}, \\ I_2 &\approx \frac{1}{R_T}(V - V_T), \\ I_1 &= I_2 = -\frac{1}{R}\frac{\partial V}{\partial x} = \frac{1}{R_T}(V - V_T). \end{aligned} \tag{16}$$

In Table 3, the modelling of boundary conditions of the heat transfer problems in TLM is summarized.

SIMULATIONS AND RESULTS

In the simulation a 1D bioelectromagnetic problem is considered. In the problem a 1D multilayer human body tissue model selected for the study. The multilayer human body tissue model used in this work is shown in Figure 7. The model consists of skin, fat, and muscle tissues, with thicknesses of 1 mm, 4 mm, and 10 mm, respectively (Lin 1986).

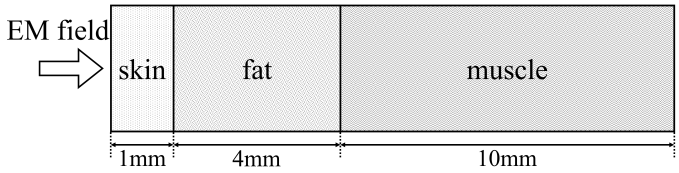

Figure 7 Multilayer human body tissue model.

In this section, the resulting temperature rise due to EM exposure in a one-dimensional (1D) multilayered human body tissue model were obtained using both the Transmission Line Modelling (TLM) method and the Finite Element Method (FEM). For the tissue model presented in Figure 7, the distribution of EM fields within the tissues was calculated at various 4G frequencies. The carrier frequencies considered were 700 MHz, 900 MHz, 1800 MHz, 2100 MHz, and 2600 MHz. The incident electric field intensity was

Table 3 The relationship between boundary conditions and the parameters of the TLM models.

	TLM	Heat Transfer Problem
Interface Boundary Condition	V_1	T_1
	V_2	T_2
	$1/R_1$	k_1
	$1/R_2$	k_2
Dirichlet Boundary Condition (Constant Surface Temperature)	V_D	T_D
Neumann Boundary Condition	I_N	q_y
Adiabatic Boundary Condition	Open Circuit	$q_y = 0$
Convection Boundary Condition	V_T	T_T
	$1/R_T$	h

set to 10 V/m for all 4G frequencies. This selected field intensity is below the general public exposure limits specified by the ICNIRP (International Commission on Non-Ionizing Radiation Protection) guidelines for all the given frequencies (ICNIRP 2009). The exposure duration used in the temperature rise calculations was set to 2 hours.

Figure 8 shows the simulation setup for the 1D bioelectromagnetic problem. In the figure, the lossy transmission lines labelled T_{Si}, T_{Fj}, and T_{Mk} represent the skin, fat, and muscle tissues, respectively. In the simulation, the skin tissue is divided into 10 equal segments, the fat tissue into 6 equal segments, and the muscle tissue into 4 equal segments. The lengths of the TLM cells representing the skin, fat, and muscle tissues are 0.1 mm, 0.67 mm, and 1 mm, respectively. The impedance, denoted as Z_L in the figure, is chosen to be as open circuit. In other words, the simulation is terminated with adiabatic boundary condition for simplicity.

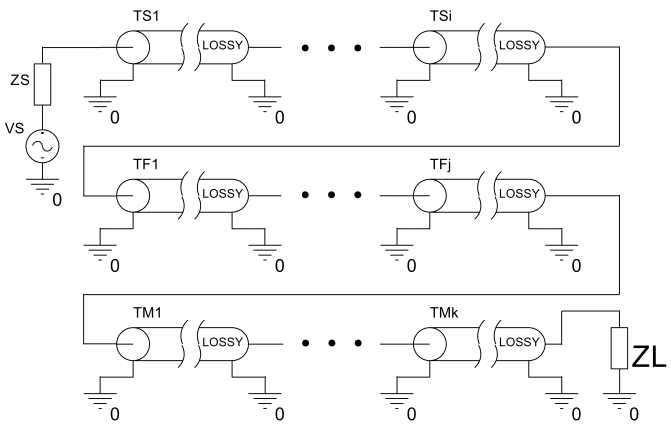

Figure 8 The simulation setup for the 1D bioelectromagnetic problem.

The average temperature rise in the body tissue model after 2 hours of exposure to the EM field is shown in Figure 9. In Figure 9, the temperature rise calculation is performed using both the TLM method and the FEM method. Additionally, the ambient temperature is chosen to be 25°C for the temperature rise calculations.

When the results of both methods are compared, the temperature rises obtained by both methods are quite similar. The total average temperature rise in the tissue model decreases monotonically with frequency at 4G frequencies. Even in the worst-case scenario, the total average temperature rise is less than 0.1°C ($\approx$ 0.07°C).

Figure 10 shows the temperature increases at both boundaries of the muscle tissue in the analyses conducted using the Klinger bioheat transfer equation-based FEM and TLM, the Pennes bioheat transfer equation-based TLM method at 2600 MHz. The muscle tissue was selected for this analysis because it is the thickest layer in the model.

As seen in Figure 10, the temperature increases at both boundaries of the muscle tissue appear to be very similar between the Klinger bioheat transfer equation-based TLM and the FEM method, particularly in the steady-state condition. The temperature difference at both and of the muscle tissue is about 1m°C. On the other hand, the results obtained using the Pennes bioheat transfer equation-based TLM show nearly identical temperature increases at both ends of the muscle tissue. This difference arises because the effect of blood flow velocity on temperature variation is neglected in the Pennes bioheat transfer equation. As a result, more accurate results were obtained using the newly developed Klinger bioheat transfer equation-based TLM.

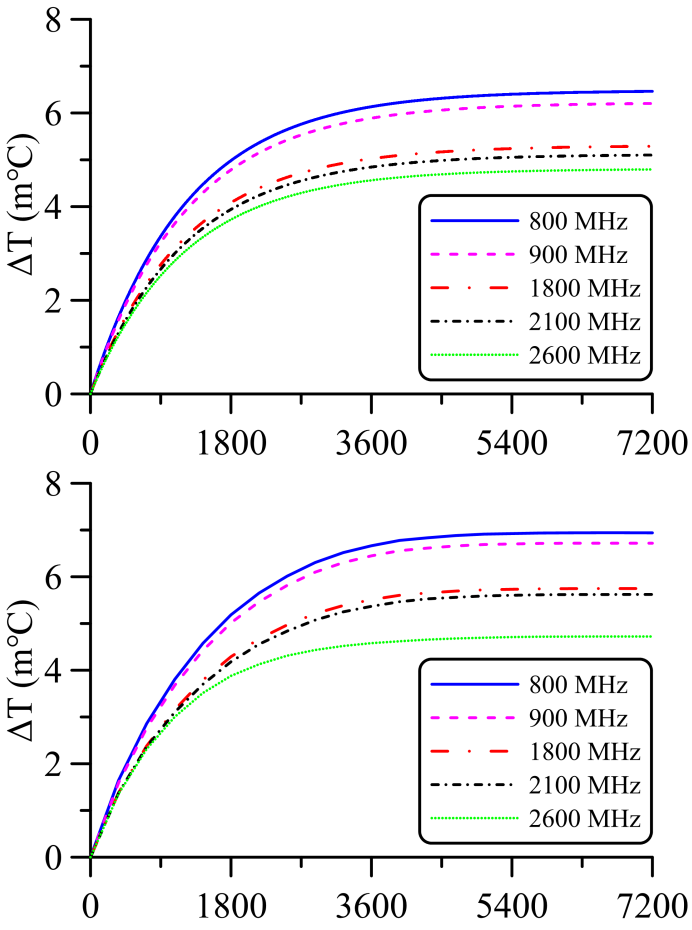

Figure 9 The average temperature rise due to exposure to 4G frequencies in a multilayered tissue model (top) TLM based method, (bottom) FEM based method.

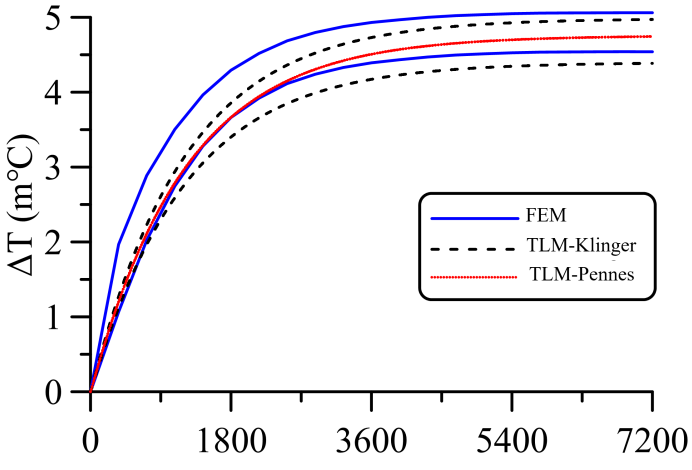

Figure 10 Temperature increases obtained at observations points in the muscle tissue using the Klinger and Pennes bioheat transfer equations-based FEM and the TLM method.

CONCLUSION

In this study, a modified Transmission Line Modelling (TLM) method was developed and applied to bioheat transfer problems by incorporating the effects of non-unidirectional blood flow through the Klinger bioheat equation. The method was validated through simulations of a multilayer human body tissue model exposed to 4G electromagnetic fields, with temperature rise predictions compared against those from the Finite Element Method (FEM). The results demonstrate strong agreement between the proposed TLM method and FEM, especially under steady-state conditions. While the Pennes-based TLM model showed nearly symmetric temperature distributions, the Klinger-based TLM method captured directional differences at tissue boundaries, underscoring the importance of modelling convective transport. The observed total average temperature rise remained below critical safety thresholds in all test cases, supporting compliance with ICNIRP exposure guidelines.

However, several limitations must be acknowledged. The assumption of homogeneous tissue properties simplifies the geometry and may not fully capture the complexities of real biological structures. Additionally, the model neglects temperature-dependent perfusion, which can influence thermal behavior in vivo. Despite these simplifications, the study lays important groundwork for extending TLM-based techniques to more anatomically realistic geometries and heterogeneous tissue conditions in future research. Overall, the Klinger-based TLM approach offers enhanced accuracy and flexibility for modelling complex bioheat transfer phenomena, particularly in scenarios where blood flow directionality plays a significant role.

Ethical standard

The authors have no relevant financial or non-financial interests to disclose.

Availability of data and material

Not applicable.

Conflicts of interest

The authors declare that there is no conflict of interest regarding the publication of this paper.

LITERATURE CITED

Abro, K. A., A. Atangana, and J. F. Gomez-Aguilar, 2021 An analytic study of bioheat transfer Pennes model via modern non-integers differential techniques. The European Physical Journal Plus **136**: 1–11.

Akulova, D. V., and M. A. Sheremet, 2024 Mathematical Simulation of Bio-Heat Transfer in Tissues Having Five Layers in the Presence of a Tumor Zone. Mathematics **12(5)**: 676.

Aricioglu, B., and A. Ferikoglu, 2021 Thermal Effects of 5G Frequency EM Waves on Ocular Tissue. The Applied Computational Electromagnetics Society Journal (ACES): 286–397.

Barman, C., P. Rath, and A. Bhattacharya, 2021 A non-Fourier bioheat transfer model for cryosurgery of tumor tissue with minimum collateral damage. Computer Methods and Programs in Biomedicine **200**: 105857.

Christopoulos, C., and C. Christopoulos, 1995 *The Transmission-line Modeling Method: TLM*. IEEE Press, New York, USA.

D'Alessandro, G., P. Tavakolian, and S. Sfarra, 2024 A review of techniques and bio-heat transfer models supporting infrared thermal imaging for diagnosis of malignancy. Applied Sciences **14(4)**: 1603.

Desai, R. A., A. J. Lowery, C. Christopoulos, P. Naylor, J. M. V. Blanshard, and K. Gregson, 1992 Computer modelling of microwave cooking using the transmission-line model. IEE Proceedings A (Science, Measurement and Technology) **139(1)**: 30–38.

El-Sapa, S., A. A. El-Bary, W. Albalawi, and H. M. Atef, 2024 Modelling Pennes', bioheat transfer equation in thermoelasticity with one relaxation time. Journal of Electromagnetic Waves and Applications **38(1)**: 105–121.

Ezzat, M. A., N. S. AlSowayan, Z. I. Al-Muhiameed, and S. M. Ezzat, 2014 Fractional modelling of Pennes' bioheat transfer equation. Heat and Mass Transfer **50**: 907–914.

Ferras, L. L., N. J. Ford, M. L. Morgado, J. M. Nobrega, and M. S. Rebelo, 2015 Fractional Pennes' bioheat equation: theoretical and numerical studies. Fractional Calculus and Applied Analysis **18**: 1080–1106.

Hristov, J., 2019 Bio-heat models revisited: concepts, derivations, nondimensalization and fractionalization approaches. Frontiers in Physics **7**: 189.

International Commission on Non-Ionizing Radiation Protection, 2009 ICNIRP statement on the Guidelines for limiting exposure to time-varying electric, magnetic, and electromagnetic fields (up to 300 GHz). Health Physics **97(3)**: 257–258.

Jiang, Q., 2024 Study of magnetic hyperthermia based cancer treatment using a holistic simulation framework.

Johns, P. B., 1977 Numerical modelling by the TLM method. In *Large Engineering Systems* (pp. 139–151), Pergamon.

Klinger, H. G., 1974 Heat transfer in perfused biological tissue-I: General theory. Bulletin of Mathematical Biology **36(4)**: 403–415.

Kumar, M., and K. N. Rai, 2022 Three phase bio-heat transfer model in three-dimensional space for multiprobe cryosurgery. Journal of Thermal Analysis and Calorimetry **147(24)**: 14491–14507.

Lin, J. C., 1986 Microwave propagation in biological dielectrics with application to cardiopulmonary interrogation. In *Medical Applications of Microwave Imaging* (pp. 47–58), IEEE Press.

Milan, H. F. M., and K. G. Gebremedhin, 2016 Solving bioenergetics problems with the transmission-line modeling (TLM) method. In *2016 ASABE Annual International Meeting*, (p. 1), American Society of Agricultural and Biological Engineers.

Milan, H. F., and K. G. Gebremedhin, 2018 General node for transmission-line modeling (TLM) method applied to bio-heat transfer. International Journal of Numerical Modelling: Electronic Networks, Devices and Fields **31(5)**.

Milan, H. F., C. A. Carvalho Jr., A. S. Maia, and K. G. Gebremedhin, 2014 Graded meshes in bio-thermal problems with transmission-line modeling method. Journal of Thermal Biology **45**: 43–53.

Ostadhossein, R., and S. Hoseinzadeh, 2022 The solution of Pennes' bio-heat equation with a convection term and nonlinear specific heat capacity using Adomian decomposition. Journal of Thermal Analysis and Calorimetry **147(22)**: 12739–12747.

Ostadhossein, R., and S. Hoseinzadeh, 2024 Developing computational methods of heat flow using bioheat equation enhancing skin thermal modeling efficiency. International Journal of Numerical Methods for Heat & Fluid Flow **34(3)**: 1380–1398.

Pennes, H. H., 1948 Analysis of tissue and arterial blood temperatures in the resting human forearm. Journal of Applied Physiology **1(2)**: 93–122.

Sherief, H. H., M. F. Zaky, M. F. Abbas, and S. A. Mahrous, 2024 Mathematical modeling of heat transfer in tissues with skin tumor during thermotherapy. PLOS One **19(5)**: e0298256.

Singh, M., 2024 Modified Pennes bioheat equation with heterogeneous blood perfusion: A newer perspective. International Journal of Heat and Mass Transfer **218**: 124698.

Tucci, C., M. Trujillo, E. Berjano, M. Iasiello, A. Andreozzi, and G. P. Vanoli, 2021 Pennes' bioheat equation vs. porous media approach in computer modeling of radiofrequency tumor ablation. Scientific Reports **11(1)**: 5272.

How to cite this article: Arıcıoğlu, B. and Ferikoğlu, A. A Modified Transmission Line Modelling Approach for Bioheat Transfer. *Computers and Electronics in Medicine*, 2(2), 36-42, 2025.